

TIPE2 deletion improves the therapeutic potential of adoptively transferred NK cells

Jiacheng Bi,¹ Chen Huang,¹ Xiaomeng Jin,¹ Chaoyue Zheng,¹ Yingying Huang,¹ Xiaohu Zheng,^{2,3} Zhigang Tian ,^{1,2,3,4} Haoyu Sun^{2,3}

To cite: Bi J, Huang C, Jin X, et al. *TIPE2* deletion improves the therapeutic potential of adoptively transferred NK cells. *Journal for ImmunoTherapy of Cancer* 2023;**11**:e006002. doi:10.1136/jitc-2022-006002

► Additional supplemental material is published online only. To view, please visit the journal online (<http://dx.doi.org/10.1136/jitc-2022-006002>).

Accepted 07 January 2023

ABSTRACT

Background To enhance the efficacy of adoptive NK cell therapy against solid tumors, NK cells must be modified to resist exhaustion in the tumor microenvironment (TME). However, the molecular checkpoint underlying NK cell exhaustion in the TME remains elusive.

Methods We analyzed the correlation between *TIPE2* expression and NK cell functional exhaustion in the TME both in humans and mice by single-cell transcriptomic analysis and by using gene reporter mice. We investigated the effects of *TIPE2* deletion on adoptively transferred NK cell therapy against cancers by using NK cells from NK-specific *Tipe2*-deficient mice or peripheral blood-derived or induced pluripotent stem cell (iPSC)-derived human NK cells with *TIPE2* deletion by CRISPR/Cas9. We also investigated the potential synergy of double deletion of *TIPE2* and another checkpoint molecule, *CISH*.

Results By single-cell transcriptomic analysis and by using gene reporter mice, we found that *TIPE2* expression correlated with NK cell exhaustion in the TME both in humans and mice and that the *TIPE2*^{high} NK cell subset correlated with poorer survival of tumor patients. *TIPE2* deletion promoted the antitumor activity of adoptively transferred mouse NK cells and adoptively transferred human NK cells, either derived from peripheral blood or differentiated from iPSCs. *TIPE2* deletion rendered NK cells with elevated capacities for tumor infiltration and effector functions. *TIPE2* deletion also synergized with *CISH* deletion to further improve antitumor activity in vivo.

Conclusions This study highlighted *TIPE2* targeting as a promising approach for enhancing adoptive NK cell therapy against solid tumors.

WHAT IS ALREADY KNOWN ON THIS TOPIC

⇒ NK cell exhaustion in the tumor microenvironment (TME) of solid tumors limits the therapeutic potential of adoptive NK cell therapy, whose molecular checkpoint remains elusive.

WHAT THIS STUDY ADDS

⇒ We found that *TIPE2* expression correlated with NK cell exhaustion in the TME in both humans and mice. *TIPE2* deletion endowed NK cells with elevated capacities for tumor infiltration and effector functions and promoted the antitumor activity of adoptively transferred mouse NK cells, as well as adoptively transferred human NK cells, either derived from peripheral blood or differentiated from induced pluripotent stem cells. *TIPE2* deletion also synergized with the deletion of another checkpoint molecule, *CISH*, to further improve antitumor activity in vivo.

HOW THIS STUDY MIGHT AFFECT RESEARCH, PRACTICE OR POLICY

⇒ This study suggests that targeting *TIPE2* represents a promising approach for enhancing adoptive NK cell therapy against solid tumors.

BACKGROUND

Adoptive NK cell therapy represents an important cutting-edge strategy against tumors.¹ However, tumor-associated exhaustion limits NK cell efficacy, especially in the tumor microenvironment (TME) of solid tumors.^{2–3} Under exhausted conditions, NK cells poorly accumulate in the tumor tissue and display impaired cytolytic activity and reduced effector cytokine production. NK cell exhaustion is usually accompanied by upregulation of cell surface inhibitory receptors and downregulation of cell surface

activating receptors. We previously identified a checkpoint for tumor-associated NK cells, the cell surface receptor TIGIT, whose protein expression correlates with the exhaustion and dysfunctional status of NK cells in the TME² and mediates NK cell exhaustion on interaction with its ligand(s) within the TME.⁴ However, whether intracellular molecular checkpoints also exist and function to regulate NK cell exhaustion in the TME remains elusive.

Genetic modifications have shown great potential for improving various parameters of adoptive NK cell therapy for cancers. Chimeric antigen receptors (CARs) endow NK cells with tumor-specific targeting capability.⁵ A noncleavable, high-affinity CD16 facilitates ADCC by NK cells.⁶ IL-15 receptor fusion supports NK cell survival without the need for cytokine supplementation. *CISH*



© Author(s) (or their employer(s)) 2023. Re-use permitted under CC BY-NC. No commercial re-use. See rights and permissions. Published by BMJ.

For numbered affiliations see end of article.

Correspondence to

Haoyu Sun;
haoyusun@ustc.edu.cn

Jiacheng Bi; jc.bi@siat.ac.cn

Zhigang Tian; tzg@ustc.edu.cn



deletion promotes NK cell IL-15 signaling and metabolic fitness.^{7,8} In particular, induced pluripotent stem cell (iPSC)-derived NK cells, an important strategy for producing a large number of genetically standardized single-clonal NK cells for immunotherapy, have enabled the potential for multiplex genome editing to enhance multiple parameters of NK cells to maximize improvements.⁹ However, genome editing to improve adoptive NK cell resistance to the TME has not been reported.

TIPE2 (tumor necrosis factor- α (TNF- α)-induced protein-8 like-2) is a negative regulator of antitumor immunity. Global deletion of *Tipe2* in mice suppressed xenografted tumor growth, accompanied by the loss of tumor-promoting effects of myeloid-derived suppressor cells.¹⁰ We have previously shown that NK-specific deficiency of *Tipe2* promotes NK cell maturation and the optimal functional status in the steady state¹¹ by elevating the mTOR response to IL-15.¹² NK-specific deficiency of *Tipe2* also improves the endogenous antitumor immune response. However, whether TIPE2 deficiency renders NK cells resistant to exhaustion in the TME and promotes NK cell antitumor activity has not been reported.

Here, the gene expression of TIPE2, a checkpoint molecule targeting IL-15-induced mTOR activity in NK cells, correlated with the functional exhaustion status in human tumor-associated NK cells, as shown by single-cell transcriptomic analysis. The deletion of TIPE2 in either mouse or human NK cells enhanced NK cell effector functions and rendered these NK cells more strongly controlled solid tumor growth in vivo after adoptive transfer into tumor-bearing mice. Therefore, targeting the checkpoint molecule TIPE2 might represent a promising approach for enhancing NK cell adoptive therapy against tumors.

METHODS

Mice

Tipe2^{flox/flox} mice were purchased from the Cam-Su Genomic Resource Center (Suzhou, China). *Ncr1*-iCre mice and NOD-Scid- γ c^{-/-} mice with transgenic human IL-15 expression ('NDG-hIL15') were purchased from Biocytogen (Beijing, China). NK-specific *Tipe2*-deficient mice ('*Tipe2*^{ΔNK/ΔNK} mice') were generated by crossing *Tipe2*^{flox/flox} mice with *Ncr1*-iCre mice. Age-matched and sex-matched *Tipe2*^{flox/flox} mice were used as controls (referred to as '*Tipe2*^{WT/WT} mice'). *Tipe2* reporter mice with a *Tipe2*-ires-*Egfp* knock-in cassette were generated by Cyagen (Suzhou, China). All mice used were 5–8 weeks old with a C57BL/6 background (except for NDG-hIL15) and were housed in a specific pathogen-free facility at the Shenzhen Institute of Advanced Technology, Chinese Academy of Sciences.

Cell lines

K562 cells and HCT15 cells were purchased from Cell-Bank (Shanghai, China). *Tap2*-deficient RMA84 lymphoma cells were preserved in-house.

Cell culture

Human primary NK cells were enriched from the peripheral blood mononuclear cells (PBMCs) of healthy donors by an NK cell isolation kit via a magnetic cell sorting kit from Miltenyi (Bergisch Gladbach, Germany), followed by expansion with an NK cell expansion kit from DAKWE (Shenzhen, China), according to the manufacturer's instructions. Alternatively, enriched and gene-edited or control NK cells were cultured in RPMI 1640 medium with 10% fetal bovine serum (FBS) and penicillin and streptomycin (100 IU/mL) plus 1000 IU/mL human IL-2 to determine the effects of gene editing on NK cell proliferation under more defined conditions. Under such conditions, the medium was half-changed every other day. iPSCs were cultured using the mTeSR1 plus kit from Stemcell Technologies (Vancouver, Canada). iPSC differentiation into NK cells was performed using the STEMdiffTM NK Cell Kit from Stemcell Technologies. K562 and RMA84 cells were cultured in RPMI 1640 medium with 10% FBS and penicillin and streptomycin (100 IU/mL). HCT15 cells were cultured in DMEM with 10% FBS and penicillin and streptomycin (100 IU/mL). Mouse splenic cells were cultured in RPMI 1640 medium with 10% FBS, penicillin and streptomycin (100 IU/mL), and 10 ng/mL IL-2 (PeproTech, Cranbury, USA). When indicated, an additional 10 ng/mL IL-10 (PeproTech, Cranbury, USA), 10 ng/mL TNF- α (PeproTech, Cranbury, USA), 10 ng/mL TGF- β (BioLegend, San Diego, USA), or 10 μ M H₂O₂ (Boster, Wuhan, China) was added. The use of peripheral blood from healthy donors was approved by the ethical committee of Shenzhen Institutes of Advanced Technology.

Tumor models

Groups of six mice per experiment were used. The group size ensured enough power to determine biological differences. No mice were excluded from this study, and no active randomization was applied to groups. Potential confounders were minimized by treatments performed in parallel. The investigators were not blinded to group allocation during the experiment and/or when assessing the outcome. Single-cell suspensions of RMA84, K562 or HCT15 cancer cells were injected subcutaneously into the indicated strains of mice (5 × 10⁵ cells for RMA84 per mouse or 5 × 10⁶ cells for K562 and HCT15 per mouse). Tumor size, endpoint tumor weight, infiltrating NK cell numbers and effector functions were measured, among which tumor size and endpoint tumor weight were the primary outcomes measured.

Genome editing in human NK cells

For the generation of *TIPE2*, *CISH*, or *TIPE2* & *CISH* double-deleted human NK cells, enriched NK cells from PBMCs of healthy donors were subjected to electroporation using the Lonza 4D Nucleofector as described.¹³ For the generation of single clonal *TIPE2*-deleted human iPSC-NK cells, WT human iPSCs were subjected to electroporation using the Lonza 4D Nucleofector, followed by

single clonalization through limited dilution and further screening of PCR and sequencing for single clones with frame-shift mutations in both alleles.

Western blot

The following primary antibodies were used for Western blotting: TIPE2 (Proteintech, Rosemont, USA), CIS (Boster, Wuhan, China), and β -Tubulin (Proteintech, Rosemont, USA).

Flow cytometry

Single-cell suspensions were stained with the appropriate monoclonal antibody in phosphate-buffered saline containing 5% rat serum. When necessary, intracellular staining was performed using the TrueNuclear Transcription Factor Buffer Set (BioLegend) according to the manufacturer's instructions. For detection of intracellular IFN- γ , TNF- α , or perforin expression, mouse lymphocytes were stimulated with Cell Stimulation Cocktail for 3 hours in vitro before staining with antibodies (Thermo Fisher, Waltham, USA). CytoFLEX (Beckman Coulter, Brea, USA) and FACSaria III (BD Biosciences, San Diego, USA) were used for analysis and cell sorting, with dead cells excluded by the LIVE/DEAD Fixable Violet Dead Cell Stain Kit (Invitrogen, Carlsbad, USA). Antibodies specific for mouse CD45 (30-F11), NK1.1 (PK136), mouse CD3 (17A2), mouse IFN- γ (XMG1.2), mouse TNF- α (MP6-XT22), human CD3 (UCHT1), human CD94 (DX22), human CD2 (TS1/8), human NKG2D (1D11), human NKG2C (S19005E), human NKp44 (P44-8), human NKp46 (9E2), human NKp30 (P30-15), human TRAIL (RIK-2), human FasL (NOK-1), human CD16 (3G8), human CD57 (HNK-1), human NKG2A (S19004C), human DNAM-1 (11A8), and human 2B4 (C1.7) were purchased from Biolegend (San Diego, USA). Antibodies specific for phospho-S6 (N7-548) were purchased from BD Biosciences (San Diego, USA).

Cytolytic assays

For cytolytic assays against K562 cells, Cell Trace Violet (CTV, Invitrogen, Carlsbad, USA)-labeled target cells were cocultured with NK cells at the indicated effector:target (E:T) ratios for 4 hours. After that, cell mixtures were stained with 7-AAD to determine the percentages of 7-AAD⁺ dead cells among CTV⁺ target cells.

Single-cell transcriptomic analysis

Analysis of filtered data on sorted CD45⁺CD56⁺CD3⁺CD4⁺CD8a⁺CD14⁺CD163⁺ NK cells from dissociated human melanoma lesions from GEO dataset GSM4134620¹⁴ was performed with Seurat^{15 16} by selecting highly variable genes using FindVariableGenes functions with default parameters, reducing the dimensionality by PCA, and clustering the cells using FindNeighbors(dims=1:5) and FindClusters (resolution=0.1). We then applied RunTSNE (dims=1:5) for visualization.

Statistical analysis

Statistically significant differences between two groups were determined by Student's t-tests or one-way analysis of variance (ANOVA) when appropriate, except that two-way ANOVA was used in the comparison of tumor growth. A $p < 0.05$ was considered significant in all analyses.

RESULTS

High TIPE2 expression closely correlates with the functional exhaustion of human tumor-infiltrating NK cells

Previously, we found that TIPE2 expression correlates with NK cell maturation. To start investigating the role of TIPE2 in regulating the functional exhaustion of tumor-infiltrating NK cells, single-cell RNA sequencing data on tumor-infiltrating NK cells from human melanoma lesions were projected into two dimensions by tSNE, which revealed the clustering of tumor-infiltrating NK cells into two different major subsets with a higher or a lower level of functional status (figure 1A), as well as a minor subset. Among the two major subsets, GSEA indicated that subset #0, compared with subset #1, was enriched with gene sets related to the cell cycle and NK cell cytotoxicity (figure 1B). Subset #0 expressed higher levels of genes encoding effector molecules (eg, *GZMA*, *GZMB*, *PRFI*, and *IFNG*), maturation markers (eg, *KLRG1*), activating surface receptors (eg, *NCRI*, *NCR3*, and *FCGR3A*), and essential transcription factors governing NK cell effector functions (eg, *TBX21*) than subset #1 (figure 1C,D). These results indicated that subset #1 represented a more functionally exhausted subset of tumor-infiltrating NK cells with lower effector functions. Based on these analyses, we found that *TIPE2* was expressed at a higher level in the more exhausted subset #1 (figure 1D), suggesting that *TIPE2* expression should correlate with human NK cell exhaustion in the TME. The online software Carcinoma Ecotyper from a recent study has managed to couple subsets of tumor-infiltrating lymphocytes with survival association.¹⁷ Carcinoma Ecotyper identified five subsets within tumor-infiltrating NK cells from figure 1A that have been associated with better or poorer survival in a pan-carcinoma cohort including 6475 patients (online supplemental figure S1A,B). Analysis of *TIPE2* expression in these NK cell subsets revealed that subset S1, with key features (*PRFI*^{hi}*FCGR3A*^{hi}*NCR3*^{hi}) corresponding to the *TIPE2*^{low} subset in figure 1D, was significantly correlated with better survival ($p = 0.000021$) (online supplemental figure S1A,B). Importantly, subset S1 expressed the lowest level of *TIPE2* among all five subsets. In addition, subset S4, coexpressing the marker *KLRG1* similar to the *TIPE2*^{low} subset in figure 1D, was mildly correlated with better survival ($p = 0.095$). On the other hand, subset S2 was not correlated with survival (S2, $p = 0.55$), while S3 and S5 were correlated with poorer survival (S3 $p = 0.0055$, S5 $p = 0.16$). Subset S3, which was most significantly correlated with poor survival ($p = 0.0055$), expressed the highest level of *TIPE2* among all five subsets (online supplemental figure S1A,B). Therefore, the *TIPE2*^{high}

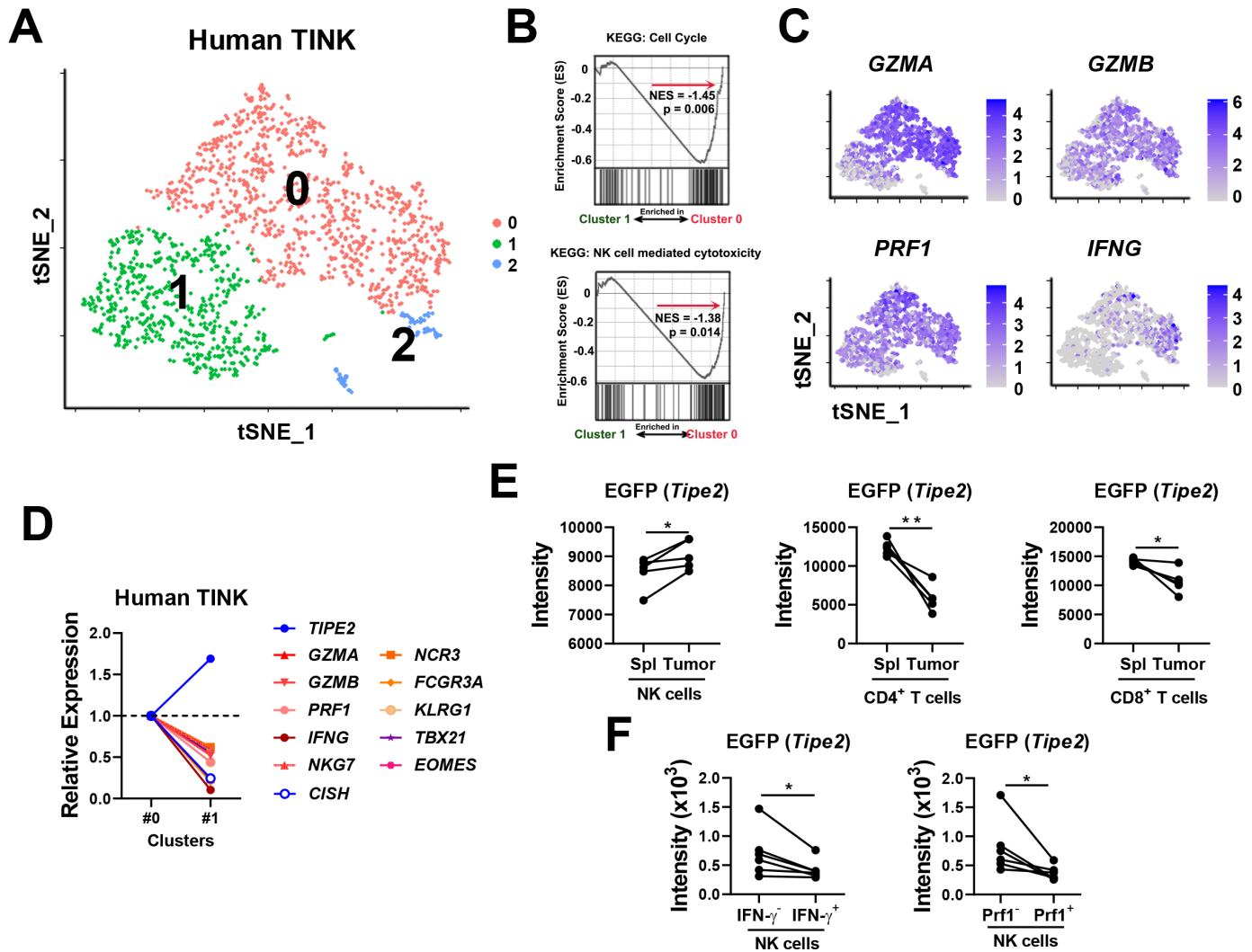


Figure 1 Correlation between *TIPE2* expression and functional exhaustion of tumor-infiltrating NK cells. (A) tSNE of human melanoma-infiltrating NK cells. (B) GSEA of subset #0 and subset #1 from (A) using KEGG: cell cycle and KEGG: NK cell-mediated cytotoxicity. (C) Feature plots showing the expression levels of the indicated genes in each cluster from (A). (D) Expression of the indicated genes in subset #1 relative to subset #0. (E, F) *Tipe2* reporter mice were subcutaneously inoculated with RMAS tumor cells. Tumor-infiltrating lymphocytes and splenic lymphocytes were analyzed from day 9 to day 14 post tumor challenge for (E) EGFP expression in different lymphocyte populations or (F) EGFP expression in tumor-infiltrating NK cells positive versus negative for IFN- γ or perforin production. (E, F) Data are representative of two independent experiments. * $p < 0.05$, ** $p < 0.005$ (paired Student's t-test).

tumor-infiltrating NK cell subset might correlate with poorer prognosis in tumor patients. On the other hand, *CISH*, a checkpoint gene involved in NK cell antitumor activity,¹⁸ was expressed at a higher level in the more functional subset #0 (figure 1D). The preferential expression of *TIPE2* and *CISH* in two different subsets with lower and higher effector functions suggests that they might function nonredundantly. Analysis of other genes involved in NK cell exhaustion, such as *HAVCR2* (Tim-3),¹⁹ *KLRG1* (NKG2A)²⁰ and *TIGIT*,⁴ showed that *KLRG1* (NKG2A) was expressed at higher levels in the more exhausted cluster, similar to *TIPE2* (online supplemental figure S2).

To confirm the correlation between the expression of *TIPE2* and NK cell exhaustion, we generated *Tipe2* reporter mice with a 'knock-in' IRES-EGFP downstream of the *Tipe2* gene open reading frame within the *Tipe2*

gene expression cassette. We established the RMAS tumor model in these mice by subcutaneous injection of 5×10^5 RMAS cells, which developed similar tumor growth as WT mice (online supplemental figure S3). Nine days later, analysis of both splenic NK cells and tumor-infiltrating NK cells showed that tumor-infiltrating NK cells expressed significantly higher levels of EGFP than splenic NK cells in the same mice (figure 1E, online supplemental figure S4A), suggesting that *Tipe2* was preferentially expressed by tumor-infiltrating NK cells. Meanwhile, such a preference was not observed in tumor-infiltrating CD4⁺ or CD8⁺ T cells (figure 1E). Moreover, IFN- γ or perforin⁻ tumor-infiltrating NK cells expressed a higher intensity of EGFP (figure 1F, online supplemental figure S4B), suggesting that *Tipe2* expression correlated with the lower functional status of tumor-infiltrating NK

cells in mice. Next, we examined several factors enriched in the TME or previously shown to upregulate TIPE2 in other cell types. We found that IL-10 increased EGFP (*Tipe2*) expression in NK cells (online supplemental figure S5). On the other hand, TNF- α /TGF- β /ROS did not significantly change EGFP (*Tipe2*) expression by NK cells. These data suggest that IL-10 might cause the upregulation of TIPE2 in the TME. Taken together, the above data indicated that TIPE2 expression correlates with NK cell exhaustion in the TME, both in humans and in mice.

***Tipe2*-deficient NK cells exert stronger therapeutic efficacy in adoptive cellular therapy against solid tumors**

Our previous study showed that *Tipe2*^{ANK/ANK} mice display enhanced control of solid tumor growth in vivo, accompanied by increased effector functions of tumor-infiltrating NK cells. Here, we further investigated whether *Tipe2* deficiency renders adoptive NK cell therapy with a better capacity for tumor control. We subcutaneously injected WT C57BL/6 mice with 5×10^5 RMAS cells. Three days later, we transferred a single dose of 2×10^5 ex vivo-stimulated WT or *Tipe2*-deficient mouse NK cells into the peritumoral region (figure 2A). The NK cells used in the transfer experiment were stimulated using IL-12, IL-15, and IL-18 to induce 'memory-like' NK cells before transfer (figure 2A). Injection of *Tipe2*-deficient NK cells significantly slowed RMAS tumor growth compared with injection of WT NK cells (figure 2B), resulting in a smaller tumor size and mass at the endpoint of the experiment (figure 2C,D). Analysis of donor-derived tumor-infiltrating NK cells showed significantly more *Tipe2*-deficient NK cells than WT NK cells (figure 2E). In addition, *Tipe2*-deficient NK cells produced higher levels of IFN- γ and TNF- α (figure 2F). These results indicated that *Tipe2* deficiency relieved exhaustion and preserved the effector functions of adoptively transferred NK cells in the TME. TIPE2 was shown to suppress mTOR activity in NK cells. Here, we found that the coinjection of rapamycin, an inhibitor of mTORC1 activity, abolished the tumor-suppressive effects of *Tipe2*-deficient NK cells (figure 2G–I). These data demonstrated that *Tipe2*-deficient mouse NK cells display improved antitumor activity in vivo in an mTOR-dependent manner.

***TIPE2*-deleted human NK cells display stronger functions in vitro**

The above results prompted us to further explore the role of TIPE2 in human NK cells. To do so, we enriched NK cells from the peripheral blood of healthy donors and deleted the *TIPE2* gene by electroporation with Cas9 protein plus a pair of guide RNAs (gRNAs) targeting the direct and complementary strands within the open reading frame of the *TIPE2* gene (figure 3A). Loss of most TIPE2 protein expression in NK cells was confirmed by western blotting (figure 3B). *TIPE2*-deleted NK cells showed enhanced proliferation in response to IL-2 stimulation in vitro (figure 3C). Meanwhile, *TIPE2*-deleted NK cells expressed similar levels of typical NK cell surface

antigens (CD16, NKp44, NKp46, NKG2D, NKG2A, KIR, TRAIL, and FasL) and maturation markers (CD94, CD2, CD57, and NKG2C) (figure 3D).

After feeder-free expansion, *TIPE2*-deleted NK cells displayed enhanced degranulation either left untreated or in response to K562 tumor cells (figure 3E). In line with this, the cytolytic activity of *TIPE2*-deleted NK cells against K562 tumor cells was stronger than that against WT NK cells (figure 3F). In addition, *TIPE2*-deleted NK cells produced significantly more IFN- γ than WT NK cells (figure 3E). These data indicated that *TIPE2*-deleted human NK cells display better effector function.

***TIPE2*-deleted human peripheral blood-derived NK cells show stronger therapeutic efficacy in solid tumor xenograft mice on adoptive cellular therapy**

To evaluate the antitumor activity of *TIPE2*-deleted human peripheral blood-derived NK cells in vivo, NDG-hIL15 mice were injected subcutaneously with 2×10^6 K562 cells. Four days later, these mice received a single injection of 10^6 WT or *TIPE2*-deleted NK cells into the peritumoral region (figure 4A). Treatment with WT NK cells significantly slowed tumor growth, while injection of *TIPE2*-deleted NK cells further enhanced tumor-suppressive effects compared with WT NK cells (figure 4B). At the endpoint, a smaller tumor burden and weight were observed in the *TIPE2*-deleted group than in the WT group (figure 4C,D). Similarly, enhanced tumor-suppressive effects of *TIPE2*-deleted NK cells were found in the HCT15 human colon tumor model (figure 4E,F). Along with the improved tumor control by *TIPE2*-deleted NK cells, we detected increased NK cells infiltrating the tumors in these mice (figure 4G,H). The tumor-suppressive effects of *TIPE2*-deleted NK cells were dose dependent, with better effects achieved using more NK cells (figure 4I). The injection time was also important, since injection of *TIPE2*-deleted NK cells at earlier time points when tumors were still smaller resulted in better therapeutic effects (figure 4J). These results indicated that stronger therapeutic effects could be achieved using adoptively transferred *TIPE2*-deleted NK cells, which results in better antitumor outcomes in vivo.

***TIPE2*-deleted human iPSC-derived NK cells show stronger therapeutic efficacy in solid tumor xenograft mice on adoptive cellular therapy**

To test whether *TIPE2* deletion would also benefit iPSC-NK cell therapy, we generated a single clonal human iPSC cell line through the electroporation of iPSCs with Cas9 protein plus the paired gRNAs of *TIPE2*, followed by screening for single clones with deletions in genomic DNA that would result in a frameshift mutation and inactivation of TIPE2 protein (figure 5A,B). WT or *TIPE2*-deleted iPSC-NK cells were generated by in vitro differentiation from WT or *TIPE2*-deleted iPSC cells to CD34⁺ hematopoietic progenitor cells and then to CD3⁺CD56⁺CD45⁺ NK cells, followed by feeder-free expansion.⁸ 10^6 Adoptively transferred *TIPE2*-deleted iPSC-NK cells significantly suppressed

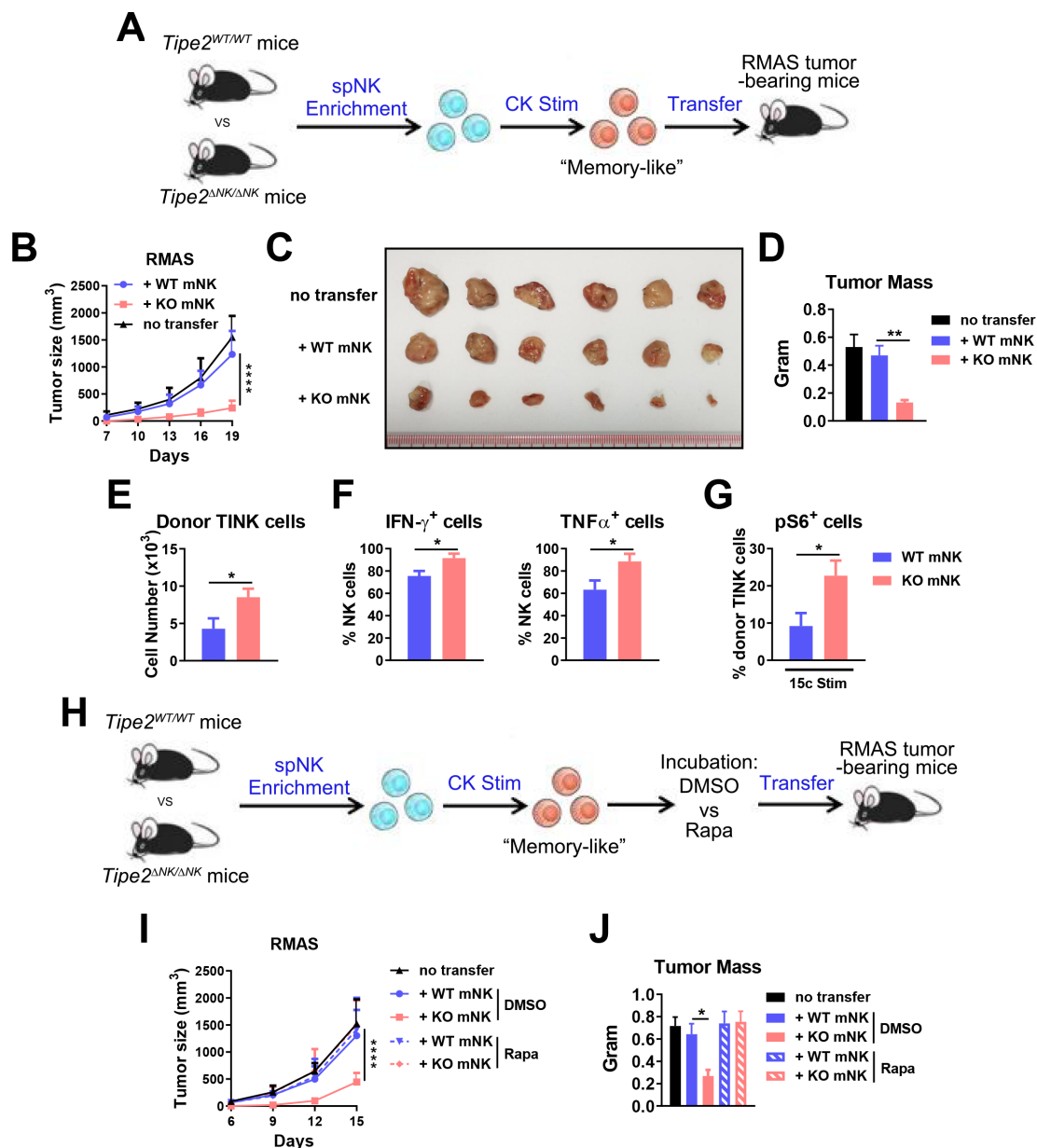


Figure 2 Antitumor activity of *Tipe2*-deficient mouse NK cells. (A) Scheme of mouse NK cell enrichment, stimulation and adoptive transfer. Mouse splenic NK cells were enriched and stimulated in vitro with 20 ng/mL IL-12, 50 ng/mL IL-15 and 10 ng/mL IL-18 for 2 days before transfer into B6 WT mice challenged with RMAS tumor cells 3 days prior. (B–D) tumor growth and endpoint tumor mass are shown for (A). (E–G) Flow cytometry analysis of tumor-infiltrating donor NK cells is shown. (E) Cell numbers per gram tumor mass. (F) IFN- γ and TNF- α production. (G) Phosphorylated S6 levels on 10 ng/mL IL-15/IL-15R α complex stimulation ex vivo. (H) Scheme of mouse NK cell enrichment, stimulation, incubation with DMSO or rapamycin, and adoptive transfer. Mouse splenic NK cells were enriched, stimulated and transferred as in (A) but with an additional in vitro incubation with 2 ng/mL rapamycin or 0.001% (v/v) DMSO for 1 hour before the transfer. (I, J) Tumor growth and endpoint tumor mass are shown for (H). (A–J) groups of 6 mice per experiment were used. data are representative of three (A–D) or two (E–J) independent experiments and are presented as the mean \pm SEM * p < 0.05, ** p < 0.005, **** p < 0.0001 (two-way ANOVA (B, I), one-way ANOVA (D, J) or unpaired Student's t -test (E–G)). ANOVA, analysis of variance.

tumor growth and displayed superior antitumor effects compared with WT iPSC-NK cells (figure 5C), resulting in a significantly smaller endpoint tumor mass (figure 5D,E). Therefore, *TIPE2* deletion also enhanced the antitumor activity of human iPSC-NK cells in vivo.

***TIPE2/CISH* double deletion greatly enhances the therapeutic efficacy of human peripheral blood-derived NK cells in solid tumor xenograft mice on adoptive cellular therapy**

We showed that *TIPE2* and *CISH* were preferentially expressed by two major subsets of human tumor-infiltrating NK cells (figure 1A). Analysis of *Cish* gene expression in *Tipe2*^{-/-} NK cells in the GSE168256 dataset we recently published showed that the *Cish* expression

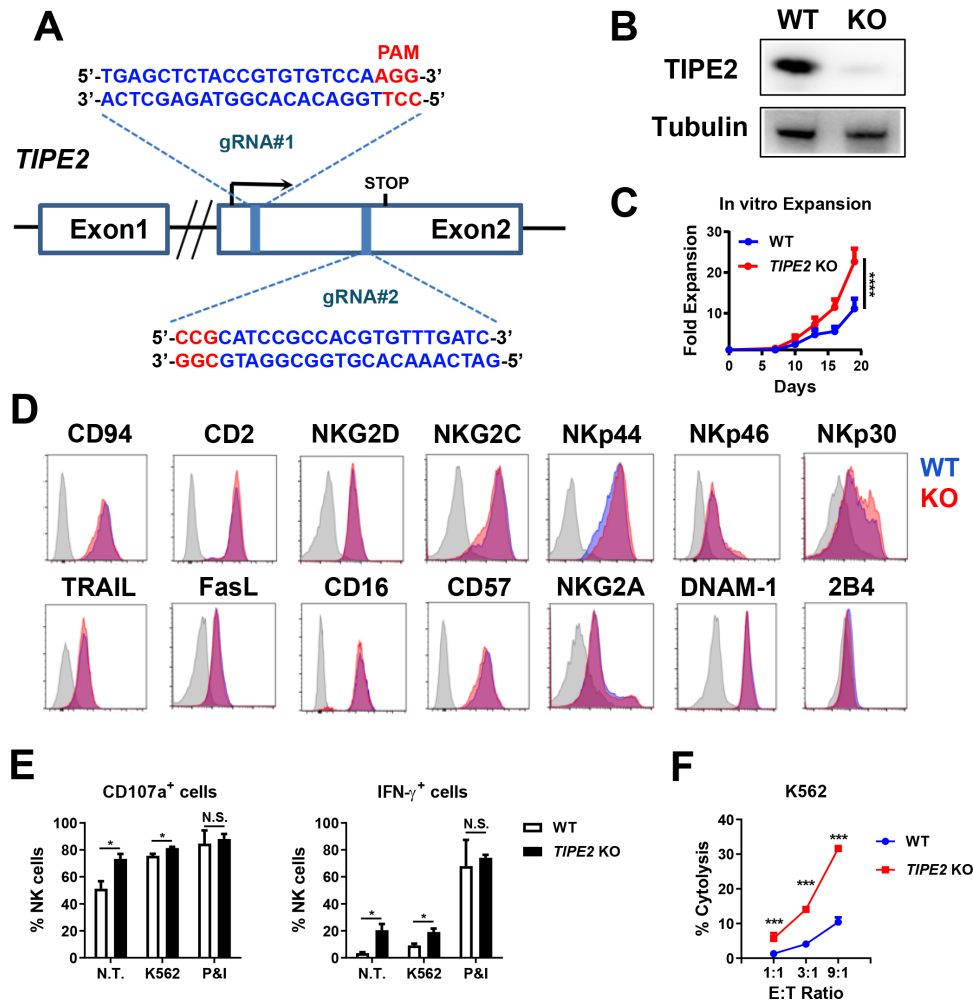


Figure 3 Phenotypic and functional analysis of *TIPE2*-deleted human NK cells. (A) Schema of CRISPR-Cas9-mediated *TIPE2* deletion using two guide RNAs (gRNAs) targeting exon 2 of the *TIPE2* gene in the direct and complementary strands. (B) Western blot analysis of *TIPE2* protein expression in WT or *TIPE2*-deleted human NK cells. (C) WT or *TIPE2*-deleted human NK cells were analyzed for IL-2-triggered proliferation in vitro. (D) Flow cytometry analysis of surface receptor expression on WT or *TIPE2*-deleted human NK cells. (E) WT or *TIPE2*-deleted human NK cells were analyzed for (left) CD107a and (right) IFN- γ expression left untreated (N.T.) or on stimulation with K562 tumor cells or PMA and ionomycin. (F) WT or *TIPE2*-deleted human NK cells were analyzed for cytolytic activity against K562 tumor cells. (B–F) Data are representative of three independent experiments. (C, E, F) Data are presented as the mean \pm SEM. * $p < 0.05$, *** $p < 0.001$, **** $p < 0.0001$, N.S. not significant. (C) two-way ANOVA. (E, F) one-way ANOVA, analysis of variance.

level was similar between wild-type and *TIPE2*^{-/-} NK cells (online supplemental figure S6), suggesting that both genes might be regulated independent of each other. We hypothesized that the deletion of both genes might relieve the functional inhibition in a larger fraction of tumor-infiltrating NK cells and further enhance their antitumor activity. Therefore, we designed a pair of gRNAs targeting the direct and complementary strands within the open reading frame of the *CISH* gene (figure 6A,B). Deletion of either *TIPE2* or *CISH* genes was performed by electroporation with Cas9 protein plus the paired gRNAs of *TIPE2*, *CISH* or both. A total of 10⁶ adoptively transferred NK cells with double deletion of *TIPE2* and *CISH* further slowed K562 tumor growth compared with NK cells with single gene deletion (figure 6C) and resulted in a significantly smaller endpoint tumor mass (figure 6D,E). These data indicated that *TIPE2* deletion synergizes with *CISH*

deletion to promote stronger antitumor activity of human NK cells than the deletion of either in vivo.

DISCUSSION

In this study, we revealed that *TIPE2* is a checkpoint molecule of tumor-infiltrating NK cells. *TIPE2* expression correlates with NK cell exhaustion in tumors. Targeting *TIPE2* in either peripheral blood-derived NK cells or iPSC-derived NK cells benefits adoptive NK cell therapy with enhanced antitumor immunity. Therefore, our study has revealed a novel checkpoint molecule of NK cell exhaustion and has shed light on resistance to immune exhaustion in tumors, a new aspect of gene modifications to improve adoptive NK cell therapy. Targeting *TIPE2* could not only synergize with targeting other checkpoint molecules (such as *CISH*) but also might be combined

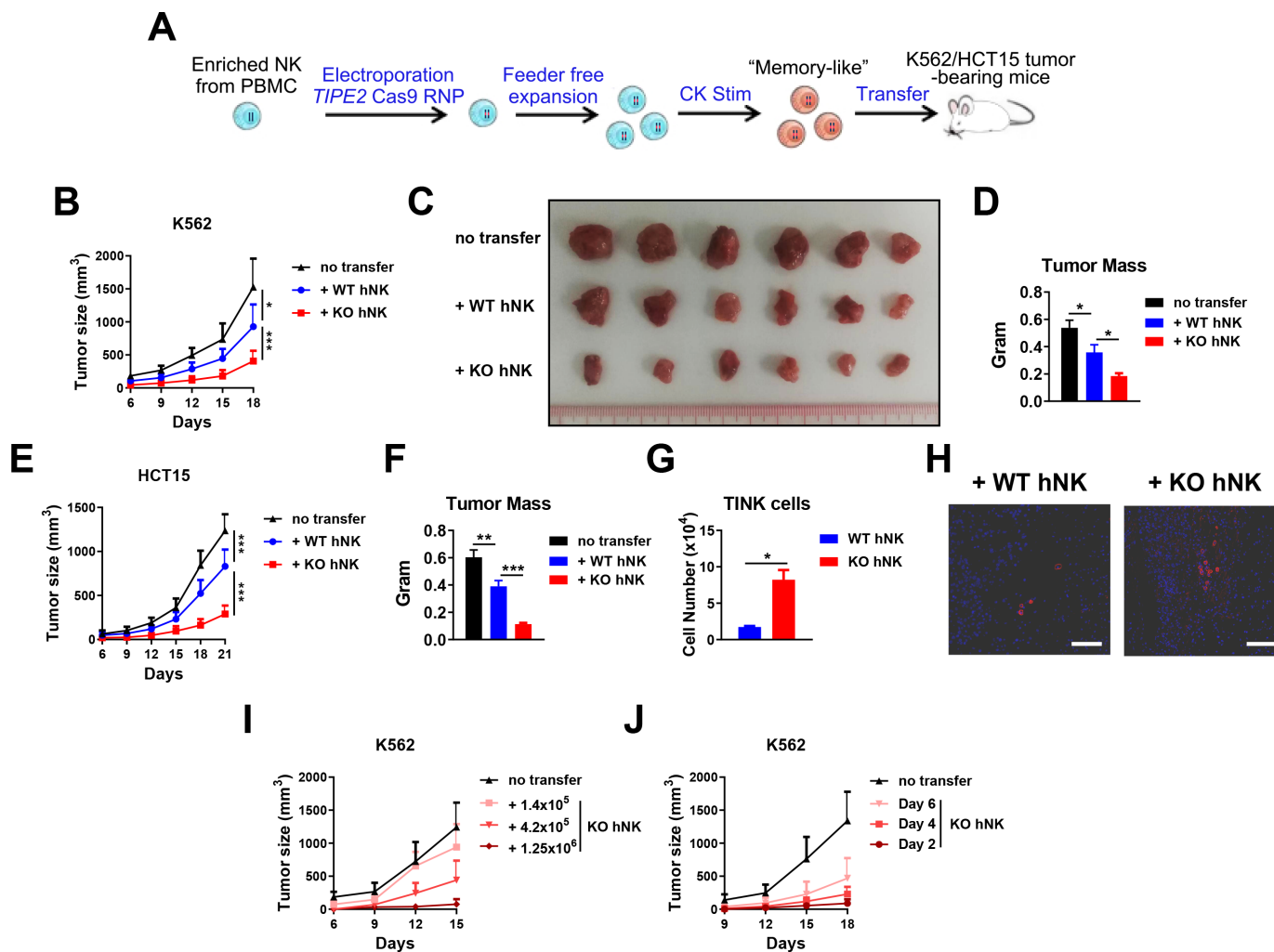


Figure 4 *TIPE2* deletion for adoptive peripheral blood-derived NK cell therapy. (A) Schematic of the generation and expansion of WT or *TIPE2*-deleted human peripheral blood-derived NK cells for adoptive transfer. NK cells were enriched from PBMCs of healthy donors and electroporated with Cas9 protein and *TIPE2*-specific gRNAs. NK cells were expanded in a feeder-free manner and stimulated with 20 ng/mL IL-12, 50 ng/mL IL-15, and 10 ng/mL IL-18 for 2 days before transfer into NDG hIL-15 mice challenged with K562/HCT15 tumor cells 3 days prior. (B–D) K562 tumor growth and endpoint tumor mass are shown for (A). (E, F) HCT15 tumor growth and endpoint tumor weight are shown for (A). (G) The numbers of K562 tumor-infiltrating human NK cells per gram tumor weight are shown for (A). (H) A representative immunofluorescent photo of the K562 tumor tissue is shown. CD56 (red) and DAPI (blue) were stained. (I) Different doses of *TIPE2*-deleted NK cells were used based on the protocol in (A). K562 tumor growth is shown. (J) Different time points of adoptive NK cell transfer post tumor challenge were selected based on the protocol in (A). K562 tumor growth is shown. (B–D) Data are representative of at least three independent experiments. (E–J) Data are representative of two independent experiments. (B–J) Groups of six mice per experiment were used. Data are presented as the mean \pm SEM. * $p < 0.05$, ** $p < 0.005$, *** $p < 0.001$. (Two-way ANOVA (B, E), one-way ANOVA (D, F), unpaired Student's t-test (G)). ANOVA, analysis of variance; PBMCs, peripheral blood mononuclear cells.

with genome modifications, such as the expression of CAR, including stable CD16 expression, IL-15 receptor fusion, and chemokine receptors, to fully release the anti-tumor potential of adoptive NK cell therapy.

The expression profile of *TIPE2* in tumor-infiltrating NK cells underlies its unique potential as a therapeutic target. *TIPE2* expression in tumor-infiltrating NK cells correlates with NK cell exhaustion in the TME, suggesting that TME-associated immunosuppressive factors might favor *TIPE2* expression. TNF- α , reactive oxygen species, IL-6, and L-arginine are abundant in the TME and have been reported to induce *TIPE2* expression.^{10,21} Here, we identified IL-10 as a positive regulator of *TIPE2* expression

in NK cells. Alternatively, the dysregulated balance of the inhibitory and activating surface receptors on NK cells in the TME that mediate NK cell exhaustion might also be *TIPE2*-inducing factors. Importantly, targeting *CISH* has been shown to improve adoptive cell therapy by NK cells from multiple sources.^{7,8} However, *TIPE2* and *CISH* seem to be expressed by NK cells from functionally distinct subsets. *CISH* expression in NK cells increases on IL-15 stimulation in vitro.¹⁸ In the TME, *CISH* was preferentially expressed in the more functional NK cell subset. On the other hand, *TIPE2* maintains steady expression in NK cells on IL-15 stimulation¹² and is expressed at a higher level by a more exhausted NK cell subset. These results suggest

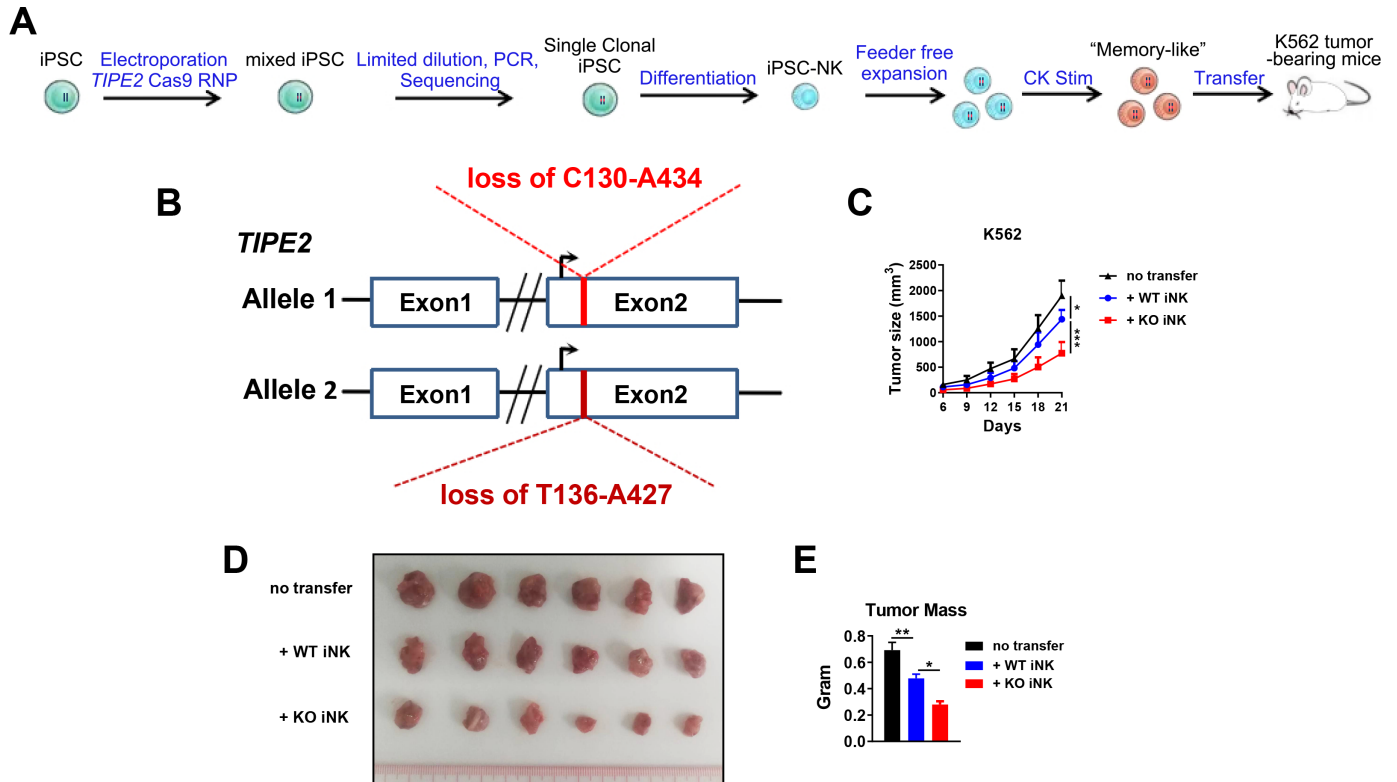


Figure 5 *TIPE2* deletion for adoptive iPSC-derived NK cell therapy. (A) Schematic of the generation and expansion of WT or *TIPE2*-deleted human iPSC-derived NK cells for adoptive transfer. iPSCs were electroporated with Cas9 protein together with *TIPE2*-specific gRNAs before single clonalization by limited dilution. Single clones were screened for *TIPE2*-deletion mutants with frame shift mutations/fragment loss. WT or *TIPE2*-deleted iPSCs were differentiated into NK cells, expanded in a feeder-free manner, and subsequently stimulated with 20 ng/mL IL-12, 50 ng/mL IL-15, and 10 ng/mL IL-18 for 2 days before transfer into NDG hIL-15 mice challenged with K562 tumor cells 3 days prior. (B) An iPSC clone with fragment loss in two *TIPE2* alleles was used in the study. Numbers indicate the position in the *TIPE2* gene open reading frame. (C–E) K562 tumor growth and endpoint tumor mass are shown for (A). Groups of six mice per experiment were used. (C, E) Data are presented as the mean \pm SEM. * $p < 0.05$, ** $p < 0.005$, *** $p < 0.001$. (Two-way ANOVA (C), one-way ANOVA (E)). ANOVA, analysis of variance; iPSCs, induced pluripotent stem cell

that *TIPE2* and *CIS* might function nonredundantly to maintain/promote exhaustion/tolerance preferentially by *TIPE2* and prevent overactivation preferentially by *CIS*. This nonredundancy offers us an opportunity to target *TIPE2* and *CISH* at the same time to relieve the suppression of NK cells in both states to maximize the improvement in NK cell therapy.

The IL-15-mTOR axis is essential for NK cell effector functions.²² Although IL-15 is expressed in the TME,²³ the activity of IL-15 signaling in tumor-associated NK cells is impaired,²⁴ resulting in the impaired effector functions of tumor-associated NK cells. Here, the absence of *TIPE2* renders adoptively transferred NK cells with elevated expression of effector functions, as well as a higher phosphorylation level of S6, indicative of higher mTORC1 activity. Inhibition of mTORC1 activity by rapamycin abrogates the improved antitumor activity of adoptively transferred *TIPE2*-deficient NK cells. These data suggest that, similar to the mode of action of *TIPE2* in the steady state, *TIPE2* might suppress NK cell activity in the TME by inhibiting the IL-15-mTORC1 axis and that preserving the activity of this axis might be essential for promoting the antitumor activity of adoptively transferred NK cells.

In this study, we employed a K562 xenograft mouse model and adoptive NK cell therapy as experimental approaches to test the therapeutic potential of *TIPE2*-deleted NK cells. In this model, K562 tumor sizes usually reach endpoints (over 1000 mm³) approximately 15–18 days post tumor injection. Therefore, we chose day 3 post tumor challenge as the NK cell transfer time when the tumor tissue started to form. Adoptive transfer of NK cells in tumor mouse models on day 3 post tumor inoculation has also been reported previously.^{25,26} In addition to transferring NK cells 3 days post tumor injection, we also tested later time points (day 4 and day 6) for NK cell transfer. Day 6 post tumor injection is the time when tumor sizes usually reach approximately 150–200 mm³ (diameters ranging from 6 to 8 mm), which represents significant tumor mass and TME formation in this model, mimicking the tumor burden of patients with late-stage cancers who might receive cancer therapies. Our results showed that transferring *TIPE2*-deleted NK cells even on day 6 post tumor injection led to an approximately 50% reduction in tumor size, demonstrating the benefits of *TIPE2* deletion on adoptively transferred NK cell therapy. Alternatively, later time points were reported using a

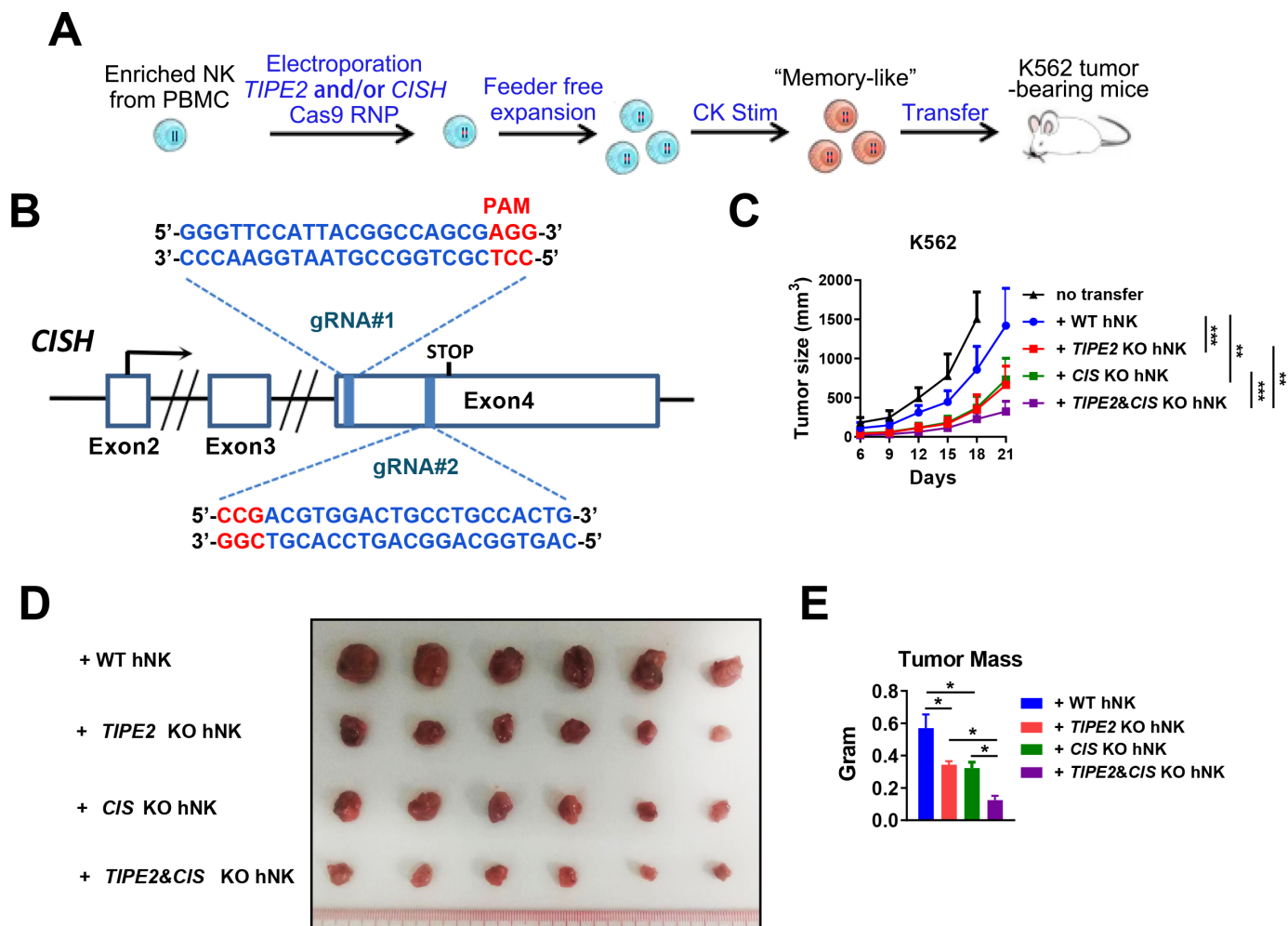


Figure 6 *TIPE2/CISH* single or double deletion for adoptive NK cell therapy. (A) Scheme of the generation and expansion of WT or *TIPE2/CISH*-single or *TIPE2/CISH* double-deleted human peripheral blood-derived NK cells for adoptive transfer. NK cells were enriched from PBMCs of healthy donors and electroporated with Cas9 protein and either one or both *TIPE2/CISH*-specific gRNAs. NK cells were expanded in a feeder-free manner and stimulated with 20 ng/mL IL-12, 50 ng/mL IL-15, and 10 ng/mL IL-18 for 2 days before transfer into NDG hIL-15 mice challenged with K562/HCT15 tumor cells 3 days prior. (B) Schema of CRISPR-Cas9-mediated *CISH* deletion using two guide RNAs (gRNAs) targeting exon 4 of the *CISH* gene in the direct and complementary strands. (C–E) K562 tumor growth and endpoint tumor mass are shown for (A). Groups of six mice per experiment were used. (C, E) Data are presented as the mean ± SEM. * $p < 0.05$, ** $p < 0.005$, *** $p < 0.001$. (Two-way ANOVA (C), one-way ANOVA (E)). ANOVA, analysis of variance; PBMCs, peripheral blood mononuclear cells.

tumor model, usually with much slower tumor growth. For example, investigators transferred NK cells on day 13 post tumor inoculation in the MDA-MB231 model in one study²⁷ when the tumor size was smaller (below 50 mm³) than that in our study. Taken together, our study supports further investigations using animal models more closely mimicking clinical conditions to evaluate the performance of *TIPE2*-deleted NK cell therapy in various tumor conditions to help us determine suitable indications.

In summary, we report that deletion of the intracellular checkpoint molecule *TIPE2* in primary NK cells from either mice or humans enhances their effector functions and antitumor activity in adoptive NK cell therapy against solid tumor models. Our study supports further clinical validation and suggests that the resistance to exhaustion in the TME through *TIPE2* deletion could be combined with tumor sensors (eg, NKR or CAR), immune checkpoint

blockade (eg, KIR, TIGIT) and synthetic gene circuits for future NK cell immunotherapy.

Author affiliations

¹The CAS Key Laboratory of Quantitative Engineering Biology, Shenzhen Institute of Synthetic Biology, Shenzhen Institute of Advanced Technology, Chinese Academy of Sciences, Shenzhen, People's Republic of China

²The CAS Key Laboratory of Innate Immunity and Chronic Disease, School of Basic Medical Sciences, Division of Life Sciences and Medicine, University of Science and Technology of China, Hefei, People's Republic of China

³Institute of Immunology, University of Science and Technology of China, Hefei, People's Republic of China

⁴Research Unit of NK Cell Study, Chinese Academy of Medical Sciences, Beijing, People's Republic of China

Contributors Conceptualization: JB, ZT and HS; Methodology: JB, CH, XJ, CZ, YH and XZ; Investigation: JB, CH, XJ, ZT and HS; Writing: JB, ZT and HS; Supervision: JB, ZT and HS; Guarantor: JB.

Funding The study was supported by grants from the National Key R&D Program of China 2020YFA0710802 (JB) and 2019YFA0508502/3 (HS) and by grants from the Natural Science Foundation of China 82071768 (JB) and 81788101 (HS).

Competing interests None declared.

Patient consent for publication Not applicable.

Ethics approval All animal experiments were approved by the Institutional Animal Care and Use Committee with the approval reference number as below: SIAT-IACUC-20220607-HCS-MYZX-BJC-A2020-01.

Provenance and peer review Not commissioned; externally peer reviewed.

Data availability statement Data are available on reasonable request. Single-cell transcriptomic analysis was based on the dataset available in the Gene Expression Omnibus (GEO) with the accession code GSM4134620.

Supplemental material This content has been supplied by the author(s). It has not been vetted by BMJ Publishing Group Limited (BMJ) and may not have been peer-reviewed. Any opinions or recommendations discussed are solely those of the author(s) and are not endorsed by BMJ. BMJ disclaims all liability and responsibility arising from any reliance placed on the content. Where the content includes any translated material, BMJ does not warrant the accuracy and reliability of the translations (including but not limited to local regulations, clinical guidelines, terminology, drug names and drug dosages), and is not responsible for any error and/or omissions arising from translation and adaptation or otherwise.

Open access This is an open access article distributed in accordance with the Creative Commons Attribution Non Commercial (CC BY-NC 4.0) license, which permits others to distribute, remix, adapt, build upon this work non-commercially, and license their derivative works on different terms, provided the original work is properly cited, appropriate credit is given, any changes made indicated, and the use is non-commercial. See <http://creativecommons.org/licenses/by-nc/4.0/>.

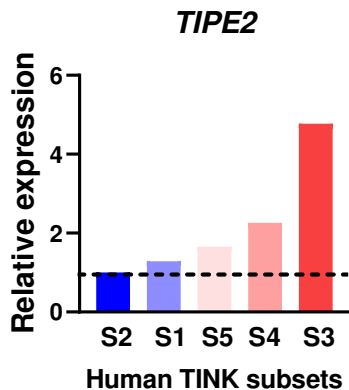
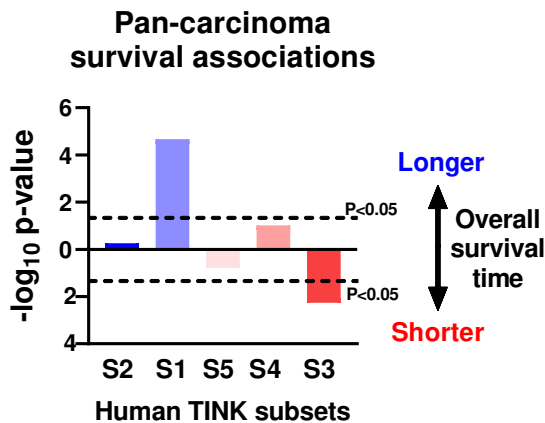
ORCID iD

Zhigang Tian <http://orcid.org/0000-0002-5512-6378>

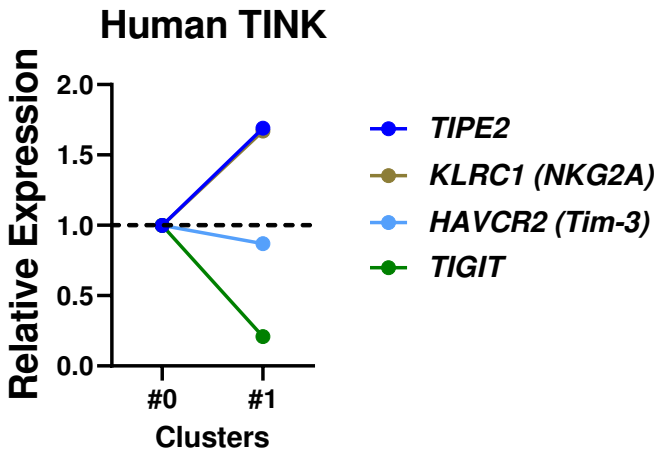
REFERENCES

- Laskowski TJ, Biederstädt A, Rezvani K. Natural killer cells in antitumor adoptive cell immunotherapy. *Nat Rev Cancer* 2022;22:557–75.
- Bi J, Tian Z. Nk cell exhaustion. *Front Immunol* 2017;8:760.
- Habif G, Crinier A, André P, et al. Targeting natural killer cells in solid tumors. *Cell Mol Immunol* 2019;16:415–22.
- Zhang Q, Bi J, Zheng X, et al. Blockade of the checkpoint receptor TIGIT prevents NK cell exhaustion and elicits potent anti-tumor immunity. *Nat Immunol* 2018;19:723–32.
- Xie G, Dong H, Liang Y, et al. CAR-NK cells: a promising cellular immunotherapy for cancer. *EBioMedicine* 2020;59:102975.
- Zhu H, Blum RH, Bjordahl R, et al. Pluripotent stem cell-derived NK cells with high-affinity noncleavable CD16a mediate improved antitumor activity. *Blood* 2020;135:399–410.
- Daher M, Basar R, Gokdemir E, et al. Targeting a cytokine checkpoint enhances the fitness of armored cord blood CAR-NK cells. *Blood* 2021;137:624–36.
- Zhu H, Blum RH, Bernareggi D, et al. Metabolic reprogramming via deletion of CISH in human ipsc-derived NK cells promotes in vivo persistence and enhances anti-tumor activity. *Cell Stem Cell* 2020;27:224–37.
- Zhu H, Kaufman DS. Engineered human pluripotent stem cell-derived natural killer cells: the next frontier for cancer immunotherapy. *Blood Sci* 2019;1:4–11.
- Yan D, Wang J, Sun H, et al. TIPE2 specifies the functional polarization of myeloid-derived suppressor cells during tumorigenesis. *J Exp Med* 2020;217:e20182005.
- Bi J, Wang X. Molecular regulation of NK cell maturation. *Front Immunol* 2020;11:1945.
- Bi J, Cheng C, Zheng C, et al. TIPE2 is a checkpoint of natural killer cell maturation and antitumor immunity. *Sci Adv* 2021;7:eabi6515.
- Rautela J, Surgenor E, Huntington ND. Drug target validation in primary human natural killer cells using CRISPR RNP. *J Leukoc Biol* 2020;108:1397–408.
- de Andrade LF, Lu Y, Luoma A, et al. Discovery of specialized NK cell populations infiltrating human melanoma metastases. *JCI Insight* 2019;4:e133103.
- Stuart T, Butler A, Hoffman P, et al. Comprehensive integration of single-cell data. *Cell* 2019;177:1888–902.
- Butler A, Hoffman P, Smibert P, et al. Integrating single-cell transcriptomic data across different conditions, technologies, and species. *Nat Biotechnol* 2018;36:411–20.
- Luca BA, Steen CB, Matusiak M, et al. Atlas of clinically distinct cell states and ecosystems across human solid tumors. *Cell* 2021;184:5482–96.
- Delconte RB, Kolesnik TB, Dagley LF, et al. Cis is a potent checkpoint in NK cell-mediated tumor immunity. *Nat Immunol* 2016;17:816–24.
- da Silva IP, Gallois A, Jimenez-Baranda S, et al. Reversal of NK-cell exhaustion in advanced melanoma by Tim-3 blockade. *Cancer Immunol Res* 2014;2:410–22.
- Sun C, Xu J, Huang Q, et al. High NKG2A expression contributes to NK cell exhaustion and predicts a poor prognosis of patients with liver cancer. *Oncotarget* 2017;6:e1264562.
- Sun H, Gong S, Carmody RJ, et al. TIPE2, a negative regulator of innate and adaptive immunity that maintains immune homeostasis. *Cell* 2008;133:415–26.
- Nandagopal N, Ali AK, Komal AK, et al. The critical role of IL-15-PI3K-mTOR pathway in natural killer cell effector functions. *Front Immunol* 2014;5:187.
- Santana Carrero RM, Beceren-Braun F, Rivas SC, et al. Il-15 is a component of the inflammatory milieu in the tumor microenvironment promoting antitumor responses. *Proc Natl Acad Sci U S A* 2019;116:599–608.
- Richards JO, Chang X, Blaser BW, et al. Tumor growth impedes natural-killer-cell maturation in the bone marrow. *Blood* 2006;108:246–52.
- Hu S, Yang J, Shangguan J, et al. Natural killer cell-based adoptive transfer immunotherapy for pancreatic ductal adenocarcinoma in a *Kras^{LSL-G12D} p53^{LSL-R172H} Pdx1-Cre* mouse model. *Am J Cancer Res* 2019;9:1757–65.
- Assmann N, O'Brien KL, Donnelly RP, et al. Srebp-controlled glucose metabolism is essential for NK cell functional responses. *Nat Immunol* 2017;18:1197–206.
- Choi SH, Kim HJ, Park JD, et al. Chemical priming of natural killer cells with branched polyethylenimine for cancer immunotherapy. *J Immunother Cancer* 2022;10:e004964.

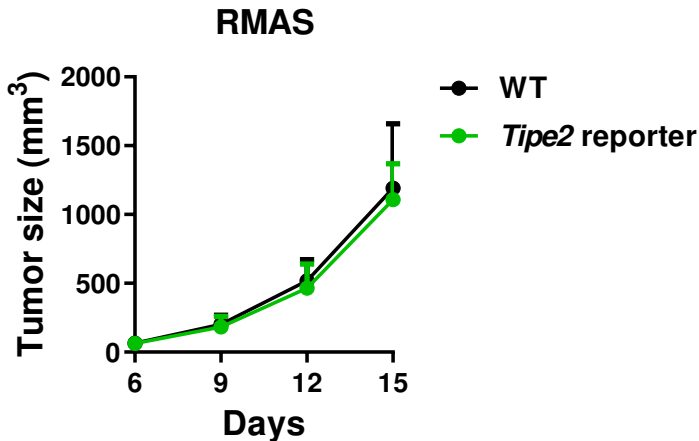
Supplemental Figure S1

A**B**

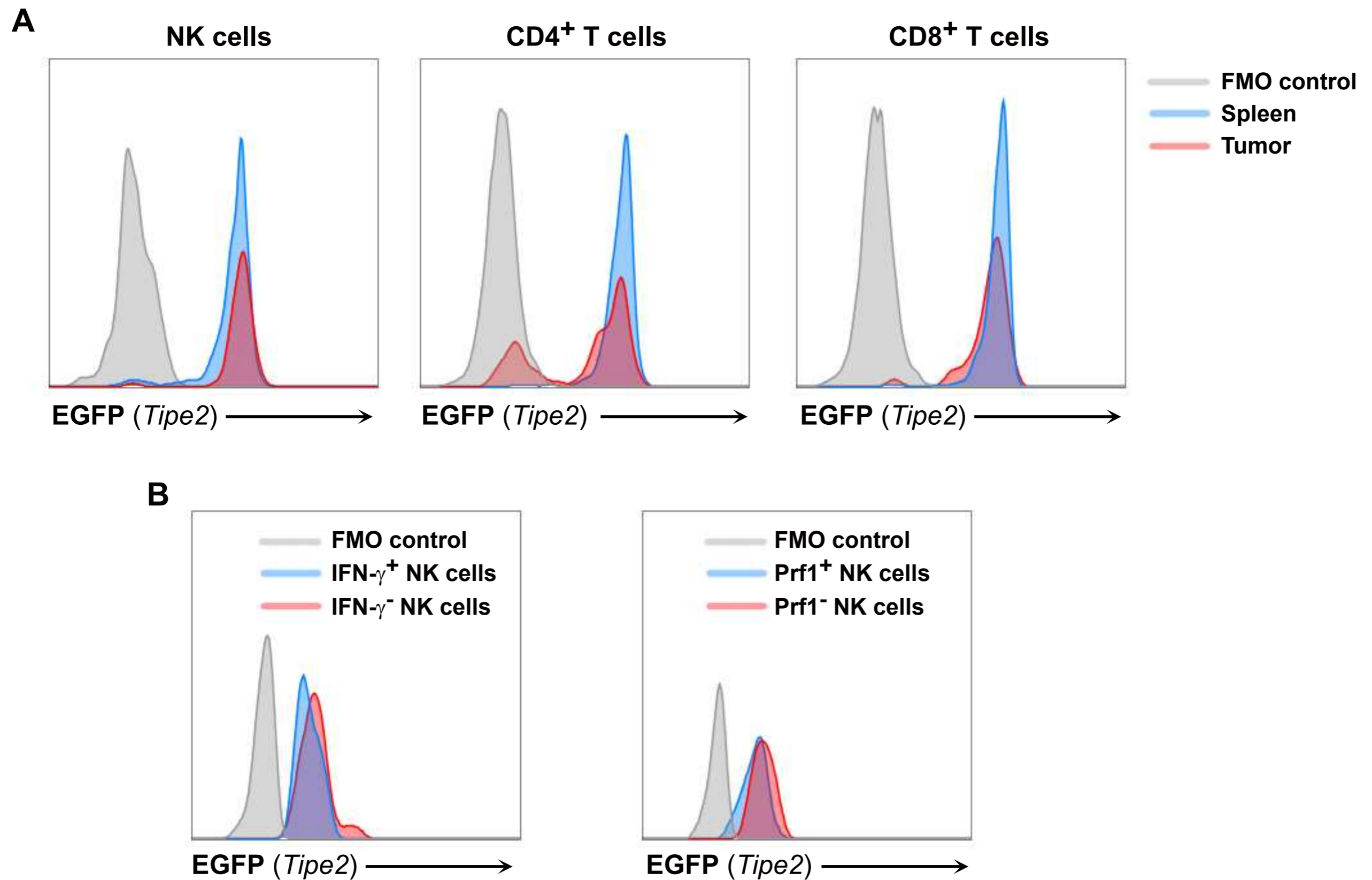
Supplemental Figure S2

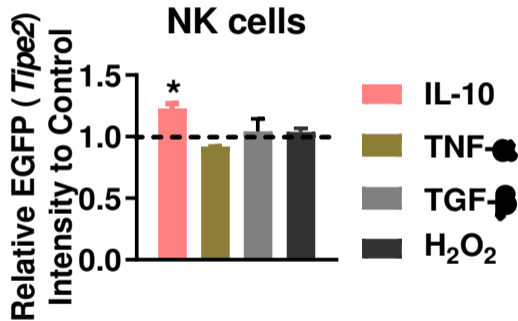


Supplemental Figure S3



Supplemental Figure S4





Supplemental Figure S6

